Published in final edited form as:
Cancer Cell. 2013 August 12; 24(2): 213–228. doi:10.1016/j.ccr.2013.06.014.

Hexokinase 2 is required for tumor initiation and maintenance and its systemic deletion is therapeutic in mouse models of cancer

Krushna C. Patra[1], **Qi Wang**[1], **Prashanth T. Bhaskar**[1], **Luke Miller**[1], **Zebin Wang**[1], **Will Wheaton**[2], **Navdeep Chandel**[2], **Markku Laakso**[3], **William J. Muller**[4], **Eric L. Allen**[5], **Abhishek K. Jha**[5], **Gromoslaw A. Smolen**[5], **Michelle F. Clasquin**[5], **Brooks Robey**[6,7], and **Nissim Hay**[1,8,*]

[1]Department of Biochemistry and Molecular Genetics, College of Medicine, University of Illinois at Chicago, Chicago, IL 60607, USA [2]Department of Medicine, Division of Pulmonary and Critical Care Medicine, Northwestern University Medical School, Chicago, IL 60611, USA [3] Department of Medicine, University of Eastern Finland, Kuopio, Finland [4]Department of Biochemistry, Goodman Cancer Research Centre, McGill University, Montreal, Quebec H3A 1A3, Canada [5]Agios Pharmaceuticals, 38 Sidney Street, Cambridge, MA 02139, USA [6]Veterans Affairs Medical Center, White River Junction, VT 05009, USA [7]Geisel School of Medicine at Dartmouth Medical School, Hanover, NH 03755, USA [8]Research & Development Section, Jesse Brown VA Medical Center, Chicago, IL 60612, USA

Summary

Accelerated glucose metabolism is a common feature of cancer cells. Hexokinases catalyze the first committed step of glucose metabolism. Hexokinase 2 (HK2) is expressed at high level in cancer cells, but only in a limited number of normal adult tissues. Using *Hk2* conditional knockout mice, we showed that HK2 is required for tumor initiation and maintenance in mouse models of KRas-driven lung cancer, and ErbB2-driven breast cancer, despite continued HK1 expression. Similarly HK2 ablation inhibits the neoplastic phenotype of human lung and breast cancer cells in vitro and in vivo. Systemic *Hk2* deletion is therapeutic in mice bearing lung tumors without adverse physiological consequences. *Hk2* deletion in lung cancer cells suppressed glucose-derived ribonucleotides and impaired glutamine-derived carbon utilization in anaplerosis.

Introduction

Accelerated glucose metabolism under aerobic conditions is one of the hallmarks of cancer cells. The elevated glucose metabolism is required to provide sufficient amounts of metabolic intermediates to support anabolic processes such as nucleic acid, lipid, and protein synthesis in the rapidly dividing cancer cells (reviewed in (Lunt and Vander Heiden, 2011; Schulze and Harris, 2012)). The dependency of cancer cell proliferation on accelerated glucose metabolism distinguishes them from their normal counterparts and could render

[*]**Corresponding Author: Nissim Hay**nhay@uic.edu.

Other detailed experimental procedures are described in the supplementary information.

them more vulnerable to the disruption of glucose metabolism. Therefore, cancer cells could be selectively targeted by the disruption of intracellular glucose metabolism. However, it unclear whether it is feasible to inhibit enzymatic activities required for glucose metabolism, at the organism level, and to selectively target cancer cells without adverse physiological consequences. The identification of isoform-specific contributors to cancer cell glucose metabolism that could be selectively targeted to disadvantage cancer cells without compromising systemic homeostasis or corresponding metabolic functions in normal cells could make such an approach feasible.

Hexokinases (HKs) catalyze the first committed step in glucose metabolism, i.e. the ATP dependent phosphorylation of glucose (Glc) to yield glucose-6-phosphate (G6P). Four major hexokinase isoforms, encoded by separate genes, are expressed in mammalian tissues—denoted as HK1, HK2, HK3, and HK4 (also known as glucokinase) (Robey and Hay, 2006). By catalyzing the phosphorylation of Glc to G6P, hexokinases promote and sustain a concentration gradient that facilitates glucose entry into cells and the initiation of all major pathways of glucose utilization. Therefore hexokinases influence both the magnitude and the direction of glucose flux within cells. Although the four HKs share many common biochemical properties, their intrinsic enzymatic activity and their tissue distribution distinguishes them from each other. HK1, HK2, and HK3 are high affinity isoforms, but HK3 is inhibited by physiological concentrations of glucose (Wilson, 2003). The high affinity hexokinases are inhibited by excess of G6P. Glucokinase is a low affinity hexokinase, which is not inhibited by G6P and is mainly expressed in liver and pancreas. The two high affinity hexokinases, HK1, and HK2, are associated with mitochondria and were also implicated in cell survival (Gottlob et al., 2001; Majewski et al., 2004). HK1 is constitutively expressed in most mammalian adult tissues. HK2, however, although is abundantly expressed in embryonic tissues, is expressed at high levels only in limited number of adult tissues such as adipose, skeletal, and cardiac muscles (Wilson, 2003). However, cancer cells express high levels of HK2 (Mathupala et al., 2001; Shinohara et al., 1994), which distinguishes them from the normal cells, and which is, at least in part responsible for the accelerated glucose flux. The high level of HK2 expression and activity in glycolytic cancers is manifested by the use of positron emission tomography (PET) to visualize tumors. PET is used following injection of the labeled glucose analog, [^{18}F] fluoro-2-deoxyglucose (FDG), which is then taken up by glycolytic cancer cells and phosphorylated by hexokinase to form FDG-phosphate, which can be detected by PET. The phosphorylation by hexokinase is required for the retention of FDG in the cancer cells. Given its selective overexpression in cancer cells, and its restricted distribution of expression in normal adult tissues, HK2 constitutes an attractive potential selective target for cancer therapy.

The studies described here are aimed at elucidating the role of HK2 in tumor initiation and maintenance of KRas-driven non-small cell lung cancer (NSCLC) and ErbB2-driven breast cancer; and to provide a proof of concept that HK2 can be systemically deleted for cancer therapy with no adverse physiological consequences.

Results

HK2 is required for oncogenic transformation

Germline deletion of *Hk2* in the mouse causes early embryonic lethality (Heikkinen et al., 1999). Therefore, we employed $Hk2^{flox/flox}$ ($Hk2^{f/f}$) mice for our studies (Fig. S1A). Mouse embryonic fibroblasts (MEFs) generated from these mice were immortalized with dominant-negative p53 (DNp53), and were subjected to adenovirus expressing Cre recombinase (Ad-Cre) infection to delete *Hk2* and to generate $Hk2^{-/-}$ MEFs (Fig. 1A). To determine the requirement of HK2 for oncogenic transformation, the cells were subjected to oncogenic

Ras. Interestingly, oncogenic Ras expression markedly elevated HK2 expression (Fig. 1A), and both PI3K and MAPK signaling contributes to this elevated expression (Fig. S1B). *Hk2* deletion impaired oncogenic transformation as measured by anchorage-independent growth on soft agar (Fig. S1C). Notably, *Hk2* deletion by Cre was not complete and a residual expression of HK2 is still observed especially in the presence of activated Ras (Fig 1A). Furthermore, the cells also express HK1 and therefore total hexokinase activity in the Ras-transformed cells was reduced by about 70% and glucose consumption was reduced by about 50% (Figs. 1B, C), and without a compensatory expression of the glucose transporter, GLUT1 (Fig. S1D). However, the deletion of *Hk2* after the expression of oncogenic Ras was sufficient to profoundly reverse oncogenic transformation (Fig. 1D). Finally, *Hk2* deletion in oncogenic Ras transformed cells markedly impaired tumor growth in vivo in xenograft assays (Fig. 1E). Re-expression of WT HK2 in $Hk2^{-/-}$ MEFs restored their susceptibility to tumorigenesis in vivo, while a kinase-dead mutant of HK2 could not (Figs. 1F, S1E and S1F). Thus, both HK2 expression and activity are required for oncogenic transformation of MEFs, and cannot be compensated by the presence of physiological level of HK1.

HK2 is required for lung and breast cancer development in mouse models

The results described above employed MEFs, which normally express HK2. However, although HK2 is expressed at relatively high levels in embryonic tissues, the major expression in adult tissues is largely restricted to muscle and adipose (Wilson, 2003). To address the role of HK2 in tumorigenesis in adult tissues in vivo, we employed mouse models of NSCLC induced by activated KRas, and a mouse model for breast cancer induced by activated ErbB2/Neu. KRas is an oncogenic driver of human NSCLC and ErbB2/neu is an oncogenic driver of human breast cancer. We first isolated lungs tissues from control WT or tumor bearing KRas mutant mice. Normal lungs express HK1 but do not express detectable HK2 protein. In contrast, HK2 protein expression was markedly elevated in the individual tumors isolated from KRas induced mice lung tumors, without any significant change in HK1 protein level (Figure 2A). We therefore employed $KRas^{LSL\text{-}G12D}$ mice, a well-characterized mouse model for NSCLC (Jackson et al., 2001). We crossed $KRas^{LSL\text{-}G12D}$ mice with $Hk2^{f/f}$ mice to generate $KRas^{LSL\text{-}G12D};Hk2^{f/f}$ mice. In these mice, exposure to Ad-Cre, through intubation, induces activated KRas expression with concomitant deletion of *Hk2*. Control $KRas^{LSL\text{-}G12D}$ and $KRas^{LSL\text{-}G12D};Hk2^{f/f}$ mice were subjected to Ad-Cre and were sacrificed 4 months after exposure to Ad-Cre. Lung tissues were isolated to determine tumor burden, individual tumor size, tumor number, proliferation and apoptosis. Total tumor burden was markedly reduced in $KRas^{LSL\text{-}G12D};Hk2^{f/f}$ mice, when compared with $KRas^{LSL\text{-}G12D}$ mice (Fig. 2B, and 2C). Moreover the average tumor size was significantly smaller in $KRas^{LSL\text{-}G12D};Hk2^{f/f}$ mice (Fig. 2D). The average number of lesions was reduced in $KRas^{LSL\text{-}G12D};Hk2^{f/f}$ mice but is not statistically significant (Fig. 2E). This effect of *Hk2* deletion is largely due to impaired proliferation as measured by BrdU incorporation (Fig. 2F). No significant increase in cell death, as measured by caspase 3 cleavage, was observed (data not shown). We concluded that HK2 is required for full oncogenic KRas-driven lung tumorigenesis. Tumors isolated from the $KRas^{LSL\text{-}G12D};Hk2^{f/f}$ mice had residual expression of HK2, possibly due to incomplete deletion, but no significant change in HK1 expression was observed (Fig 2G). Taken together these results suggest that small lesions could be developed even at very low level of HK2 expression, but cannot be further develop into large tumors. This was manifested by the striking effects of *Hk2* deletion not only on $KRas^{LSL\text{-}G12D}$ mouse tumor burden, but also on overall mortality. Kaplan-Meier survival curves reveal profoundly delayed mortality of $KRas^{LSL\text{-}G12D};Hk2^{f/f}$ mice relative to $KRas^{LSL\text{-}G12D}$ mice. In addition, more than 50% of HK2-deficient $KRas^{LSL\text{-}G12D};Hk2^{f/f}$ mice were still alive 250 days following Ad-Cre exposure, a time point corresponding to 100% mortality in HK2-expressing $KRas^{LSL\text{-}G12D}$ mice (Fig. 2H).

We found that HK2 expression is also markedly elevated in tumor tissues of mouse models of breast cancer, whereas it is hardly detected in the normal mammary gland (Fig. 3A). We, therefore, crossed *MMTV-Neu-IRES-Cre (MMTV^{NIC})* mice, which co-express activated Neu and Cre in the mammary gland with *Hk2$^{f/f}$* mice. *MMTV^{NIC}* transgenic mice develop mammary gland tumors with a complete penetrance (Ursini-Siegel et al., 2008). As shown in Fig. 3B all the *MMTV^{NIC}* (*NIC;Hk2$^{+/+}$*) mice developed tumors with an onset of less than 20 weeks. *Hk2* deletion delayed the onset of tumor appearance and had a striking effect on the incidence of tumors. At the time when 100% of *NIC;Hk2$^{+/+}$* mice developed tumors more than 60% of *MMTV^{NIC}*; *Hk2$^{f/f}$* (*NIC;Hk2$^{f/f}$*) mice remained tumor free (Fig. 3B). Furthermore, when tumors isolated from *NIC;Hk2$^{f/f}$* mice were analyzed for HK2 expression, they display comparable levels of HK2 to that observed in tumors derived from *NIC;Hk2$^{+/+}$* (Fig. 3C). Thus, these tumors were originated from cells in which *Hk2* was not efficiently deleted, suggesting that if *Hk2* would be completely deleted in all the mammary cells, which express activated Neu, the outcomes would have been even more substantial.

Taken together these results provided compelling evidence that HK2 is required for both oncogenic KRas-driven lung tumorigenesis and ErbB2-driven mammary gland tumorigenesis in vivo.

HK2 ablation reverses tumorigenesis in vitro and in vivo of NSCLC and breast cancer cells

To determine if HK2 expression is also elevated in human patient samples, we analyzed tumor tissue microarray (TMA) of human NSCLC. Immunohistochemical staining showed that HK2 expression is markedly and significantly elevated in tumor samples of NSCLC when compared to adjacent normal lung tissue, and that the higher HK2 expression level is correlated with the pathological grade of the tumors (Fig. 4A). To further assess the prognostic significance of high HK2 expression in human patients we analyzed previously generated microarray dataset comprising a large number of human NSCLC patients (Shedden et al., 2008). We found that high HK2 expression is significantly ($p=0.0025$) associated with poor prognosis of these individuals (Fig. S2A). We therefore examined the ability of HK2 ablation to reverse tumorigenicity of human lung cancer cell lines. For this purpose we have generated lentiviral vector expressing *HK2*-specific shRNA, which efficiently silenced HK2 in the human cancer cells (Fig. 4B). This shRNA was selected from several other shRNAs as the most efficient one (Fig. S2B). Expression of rat HK2, which is resistant to silencing by the human HK2 shRNA, restores the proliferation of the knockdown cells, indicating that the effect of the shRNA is specific to *HK2* (Fig. S2C). Interestingly, overexpression of HK1 could also restore proliferation to some extent (Fig. S2D). All the NSCLC cell lines tested express HK1 (Fig. 4B), but the knockdown of *HK2* significantly and markedly decreased the proliferation of three human NSCLC cell lines tested despite HK1 expression (Fig. S2E). Importantly, the knockdown of *HK2* markedly attenuated the ability of all NSCLC cell lines tested to grow in an anchorage-independent manner (Fig. 4C). We then expressed doxycycline (DOX) inducible HK2 shRNA in H460 cells (Fig. 4D). The inducible knockdown reduced the proliferation rate of these cells to a similar extent as the noninducible knockdown (Fig. S2F) with a modest increase in cell death (Fig. S2G). The cells were then inoculated into nude mice. When tumors reached approximately 65mm^3 in volume, experimental mice groups were subjected to DOX in the diet. As shown in Fig. 4E, the induction of HK2 silencing by DOX substantially attenuated the growth of the tumors. We ruled out the possibility that the attenuated tumor growth is due to a potential DOX toxicity since a similar attenuated tumor growth occurred when we compared the tumor growth of cells expressing DOX-inducible HK2 shRNA to that of cells expressing DOX-inducible scrambled shRNA after DOX treatment (Fig. S2H). Tumors isolated from treated and untreated mice, at the endpoint of the study, showed no significant change in HK2 level (Fig. 4F), suggesting that the cells, which gave rise to these tumors escaped the knockdown.

We therefore analyzed the tumors one week after DOX treatment, and found a substantial silencing of HK2 expression (Fig. 4G), and reduced BrdU incorporation (Fig. 4H), further supporting that the tumors observed at a later stage were derived from cells that escaped the knockdown of *HK2*. Because of the remarkable effect of HK2 silencing on tumor growth, and because the tumors that appeared after induction of HK2 silencing escaped silencing, we predict that a more effective HK2 silencing would completely block tumor growth.

To determine if HK2 ablation could reverse the tumorigenic phenotype of the murine lung cancer cells, we crossed $KRas^{LA2\text{-}G12D}$ mice (Johnson et al., 2001) with $Hk2^{f/f}$ mice and generated cell lines derived from the lung tumors developed in these mice. These primary tumor cell lines expressed HK2 like their tumor counterparts (data not shown). The lung cancer cell lines were infected with either adenovirus expressing LacZ or Cre. Efficient deletion of *Hk2* was observed in the cells (Fig. 4I). *Hk2* deletion in $KRas^{LA2\text{-}G12D}$ cells markedly reduced the proliferation of the cells (Fig. 4J).

As in NSCLC, HK2 expression is markedly elevated in human breast cancer tissues and its expression level is correlated with the pathological stage of the tumors (Fig. 5A). Again the analysis of an available human breast cancer dataset (van de Vijver et al., 2002) showed that high HK2 expression is significantly associated with high mortality of the patients (Fig. S3A). We therefore silenced HK2 expression in multiple breast cancer cell lines (Fig. 5B), and found that it markedly affected their ability to grow in anchorage independent manner (Fig. 5C). Moreover, the knockdown of *HK2* in MDA-MB-453 breast cancer cells, which display *ERBB2* amplification, impaired their ability to form orthotopic tumors in nude mice (Fig. 5D). We concluded that HK2 ablation could reverse the tumorigenicity of human breast cancer cells in vitro and in vivo.

To determine if HK2 ablation could reverse tumorigenesis of ErbB2-driven mammary tumors, we crossed $MMTV^{NeuT}$ mice (Muller et al., 1988) with $Hk2^{f/f}$ mice and isolated mammary tumor cell lines from these mice. *Hk2* was deleted by Ad-Cre (Fig. S3B), and early passage HK2 proficient or HK2 deficient cells were subjected to orthotopic transplantation. As shown in Fig. 5E the deletion of *Hk2* dramatically attenuated tumor growth in vivo. The impaired ability of HK2 deficient cells to form tumors is due to impaired proliferation as verified by a decrease in BrdU incorporation (Figs. 5F and 5G). Thus, these results clearly show that HK2 ablation could reverse the tumorigenicity of tumor cells derived from mouse mammary tumors.

In summary, these results provided strong evidence that the induction of HK2 expression is essential for the neoplastic phenotype of lung and breast cancer cells, and that HK2 ablation reverses the tumorigenicity of these cancer cells in vitro and in vivo. This was observed in mouse models of NSCLC and breast cancer, and was recapitulated in human NSCLC and breast cancer.

Systemic *Hk2* deletion in adult mice does not cause an overt phenotype but reduces tumor burden of lung cancer

As was shown above HK2 is expressed at high levels in cancer cells but is hardly detectable in the corresponding normal tissues from which they were derived. HK2 is expressed as the predominant isoform in only limited number of adult tissues such as fat, muscles and heart (Fig. S4A), and mice with 50% deletion of *Hk2* do not show an overt phenotype except of mildly impaired glucose homeostasis in response to exercise and high fat diet (Fueger et al., 2003).

The next question that needed to be addressed is whether systemic whole body ablation of HK2 can reverse tumorigenesis without eliciting adverse physiological consequences. We

therefore crossed $Hk2^{f/f}$ mice with mice, harboring the ubiquitously expressed tamoxifen inducible Cre ($UBC^{CreERT2}$) (Ruzankina et al., 2007) in order to systemically delete *Hk2* in all adult tissues following exposure to tamoxifen. The generated $Hk2^{f/f};UBC^{CreERT2}$ mice were treated with tamoxifen when they were two month old as previously described (Ruzankina et al., 2007). As shown in Fig. 6A, *Hk2* was effectively deleted in adult tissues expressing high levels of HK2, although the deletion was incomplete in some of the tissues. Surprisingly, global HK2 ablation in adult mice was well tolerated, and HK2-deficient mice were indistinguishable from control mice both morphologically and in terms of growth and body weight (Fig. S4B). We then examined if these mice display impaired glucose homeostasis. Mice globally deficient for HK2 had normal glucose and insulin levels under both fed and fasting conditions and responded normally to glucose tolerance testing (Fig. S4C–E). These mice were continuously monitored for over two years without development of any overt distinguishing morphological or metabolic phenotypes.

To test if systemic ablation of HK2 can reverse tumorigenesis in vivo, we employed the, $KRas^{LA2\text{-}G12D}$ NSCLC mouse model, in which lung tumors are developed with an early onset and complete penetrance (Johnson et al., 2001). We intercrossed $Hk2^{f/f};UBC^{CreERT2}$ and $KRas^{LA2\text{-}G12D}$ mice to generate $KRas^{LA2\text{-}G12D};UBC^{CreERT2}$, $KRas^{LA2\text{-}G12D};Hk2^{f/f}$, and $KRas^{LA2\text{-}G12D};Hk2^{f/f};UBC^{CreERT2}$ mice. These mice were injected with tamoxifen after tumor lesions onset, at 2 months of age, to systemically delete *Hk2*. Mice were sacrificed 4 months later and lungs were analyzed for tumor burden (see schematic diagram in Fig. 6B). There was no significant difference in tumor burden among tamoxifen treated control groups $KRas^{LA2\text{-}G12D};Hk2^{f/f}$ and $KRas^{LA2\text{-}G12D};UBC^{CreERT2}$ treated with tamoxifen (Fig. S4F). However, tumor burden was substantially decreased after *Hk2* deletion in $KRas^{LA2\text{-}G12D};Hk2^{f/f};UBC^{CreERT2}$ mice as compared to $KRas^{LA2\text{-}G12D}Hk2^{f/f}$ mice (Figs. 6C and 6D). Likewise tumor numbers per mouse were significantly decreased after *Hk2* deletion (Fig. 6E). Tumor size distribution showed that the majority of tumors in the tamoxifen treated $KRas^{LA2\text{-}G12D};Hk2^{f/f};UBC^{CreERT2}$ mice are relatively smaller (Fig. 6F). Because of the stochastic nature the inducible Cre system, HK2 expression was still detectable in some tumors arising in tamoxifen-treated $KRas^{LA2\text{-}G12D};Hk2^{f/f};UBC^{CreERT2}$ mice especially in larger size tumors (Fig. 6G). Therefore, it is likely that a sub-group of the tumors that appeared in tamoxifen–injected $KRas^{LA2\text{-}G12D};Hk2^{f/,f}UBC^{CreERT2}$ mice arose from cell lineages that escaped complete *Hk2* deletion. However, in tamoxifen–injected $KRas^{LA2\text{-}G12D};Hk2^{f/f};UBC^{CreERT2}$ mice, both the small and the larger tumors display markedly impaired proliferation (Figs. 6H and S4G), indicating that even reduced HK2 expression attenuates tumor growth.

In order to characterize the tumors immediately after HK2 loss, we injected tamoxifen to 16–18 weeks old mice, at a stage in which most of the tumors express very high levels of HK2 (data not shown). One week after the last dose of tamoxifen injection, we analyzed the tumors for BrdU incorporation. We found that the tumors derived from the tamoxifen-injected $KRas^{LA2\text{-}G12D};Hk2^{f/f};UBC^{CreERT2}$ mice incorporated substantially less BrdU when compared to control mice (Fig. S4H). These results further support that HK2 is required for the proliferation of established lung tumor cells in vivo. Importantly, taken together, these observations provided compelling genetic evidence that HK2 could be an attractive target for lung cancer therapy, without adverse physiological consequences.

HK2 is required for ribonucleotides synthesis, serine biosynthesis pathway, and the flow of carbons from glycolysis into the TCA cycle and fatty acids synthesis in $KRas^{G12D}$-NSCLC cells

As demonstrated above, HK2 is specifically elevated during tumorigenesis and is required for tumorigenesis despite persistent HK1 expression. Both HK1 and HK2 are capable of phosphorylating glucose into G6P, which is then utilized and required in multiple

fundamental metabolic processes, which are essential for glycolytic and rapidly dividing cells. These include glycolysis – either coupled to, or independent of, mitochondrial oxidative metabolism – nucleotide biosynthesis via the pentose phosphate pathway (PPP), amino acid biosynthesis, lipogenesis, and hexosamine biosynthesis required for glycosylation. It is, therefore, possible that the induction of HK2 expression in cancer cells, which already express HK1, is required for the high metabolic demand of the cancer cells. To test this possibility we have established cell lines derived from lung tumors of $KRas^{LA2\text{-}G12D};Hk2^{f/f}$ mice. For long-term studies the cell lines were first infected with retrovirus expressing DNp53. Two isogenic pairs of cell lines were chosen for further analyses, and were subjected to adenovirus infection with either Ad-LacZ or Ad-Cre to delete *Hk2*. *Hk2* deletion (Fig. S5A) impaired the proliferation of the cells (Fig. S5B).

To investigate the possibility of differential utilization of glucose upon *Hk2* deletion, we then conducted metabolomics analyses of the cells using liquid chromatography tandem mass spectrometry (LC/MS/MS). Although the abundance of many metabolites were decreased by *Hk2* deletion in both cell lines (Fig. 7A), the most statistically significant decrease was found in the levels of fructose 1, 6 bisphosphate (F1,6BP) and phosphoserine (p-Ser). Differential rates of biosynthesis were then investigated by the exchange of glucose in culture medium with stable isotopes of glucose and analysis of resultant labeling patterns. Upon feeding with U-$^{13}C_6$ glucose, incorporation of glucose-derived pentose units into ribonucleotides was impaired by *Hk2* deletion (Fig. 7B). However, the labeling patterns of non-oxidative PPP intermediates, including ribose 5-phosphate, were not affected (Fig. S5C).

In a previous study in a mouse model of KRas-dependent pancreatic ductal adenocarcinoma it was shown that oncogenic KRas induces nucleotides biosynthesis largely through the enhancement of the non-oxidative branch of the PPP (Ying et al., 2012). We therefore speculate that in *Hk2* deleted cells the PPP is in a mode that does not support high generation of ribonucleotides through the non-oxidative branch of the PPP, but rather maintains G6P/F6P equilibrium and NADPH derived from the oxidative PPP. Indeed, NADP and NADPH levels were not significantly changed (Fig. 7A). Additionally the proportion of G6P shunted to the oxidative PPP is not affected by *Hk2* deletion, as demonstrated by equivalent fractions of labeled lactate containing $^{13}C_1$ upon feeding with 1,2-$^{13}C_2$ glucose (Lee et al., 1998) (Fig. 7C). In this experiment, singly labeled lactate is assumed to have been derived exclusively from the oxidative PPP, where one of the labels is lost as $^{13}CO_2$. Taken together, these strongly indicate that the oxidative branch of the PPP is not impaired in the absence of HK2. Despite *Hk2* deletion, the pool sizes of G6P/F6P are not significantly decreased. Therefore, it is possible that in the absence of HK2 more non-oxidative PPP intermediates are shunted to regenerate F6P instead of being used to generate ribonucleotides. However this possibility requires further experimental validation. Consistent with the reduced diversion of glucose into ribonucleotides synthesis in the absence of HK2, we found a significant reduction in the incorporation of both U-$^{14}C_6$ labeled glucose and 1-$^{14}C_1$ labeled glucose, the latter of which labels nucleotides derived from the non-oxidative branch of the PPP (among other routes), into DNA and RNA in the absence of HK2 (Fig. S5D).

Flow of carbon from glycolysis into the TCA cycle is also reduced upon *Hk2* knockout, as demonstrated by the reduced fraction of doubly labeled citrate/isocitrate and cis-aconitate (Figs. 7D and S5E). The pool sizes of citrate/isocitrate and cisaconitate were also significantly reduced. Notably, a reduced fraction of doubly labeled acetyl-CoA (AcCoA) is also observed. Since cytosolic and mitochondrial pools may not be differentiated by this study, AcCoA observed is a summation of the functions of both pyruvate dehydrogenase,

and ATP citrate lyase, the latter of which is en route to fatty acid biosynthesis. Reduced doubly labeled AcCoA reflects a reduction in one, or both of these fluxes.

Glutamine-derived carbon incorporation into TCA cycle intermediates is reduced in KRas^{G12D}-NSCLC cells following *Hk2* deletion

Oncogenic Ras-transformed cells are highly dependent on the availability of glutamine, which is heavily incorporated into TCA cycle intermediates in these cells (Gaglio et al., 2011). We therefore examined *Hk2* deletion for the ability to alter glutamine requirements in oncogenic Ras-expressing cells. Interestingly, we found that exogenous glutamine restriction markedly reduced proliferation of both KRas^{G12D}-NSCLC cells and MEFs transformed by oncogenic Ras. In contrast, proliferation of these cells following *Hk2* deletion was not further affected by glutamine restriction (Fig. S5F).

Across all conditions tested, it is apparent that the pool sizes of TCA cycle intermediates, and those metabolites directly adjacent, are reduced by *Hk2* deletion (Fig. 7E). To further investigate fluxes throughout the TCA cycle, cells were fed U-$^{13}C_5$ labeled glutamine. Upon conversion to glutamate (Glu) then α-Ketoglutarate (aKG), all five ^{13}C labeled carbons from glutamine (Gln) are maintained. Observed raw signal from the LC/MS/MS indicates that the 5-labeled forms of Gln and Glu are relatively similar between control and *Hk2* deletion, while a drastic drop is observed in the 5-labeled signal for aKG, suggesting that the transamination reaction of Glu to aKG is impaired by *Hk2* deletion (Fig. 7F). Although this reaction can be catalyzed by many enzymes including GDH (glutamate dehydrogenase), GOT (glutamate-aspartate aminotransferase), and ALT (alanine transaminase), it was previously reported that in cells expressing high 3-phosphoglycerate dehydrogenase (PHGDH), approximately half of aKG is generated by the transamination catalyzed by phosphoserine aminotransferase (PSAT1) in the serine biosynthesis pathway (Possemato et al., 2011). Because *Hk2* deletion reduced the abundance of p-Ser (Fig. 7A), it is possible that the effect of HK2 on the serine biosynthesis pathway also affects the utilization of Gln into aKG. Although the pool size of total unlabeled aspartate was not significantly changed upon deletion of *Hk2* (Fig. 7E), the pool size of $^{13}C_4$ aspartate derived from Gln was reduced (Fig. 7F).

Decarboxylation of aKG, derived from U-$^{13}C_5$ Gln, to succinate, fumarate, malate and aspartate yields $^{13}C_4$ carbons upon the first turn of the TCA cycle, and $^{13}C_2$ upon the second turn (Fig. S5G). In the first turn of the TCA cycle, reduced flux into succinate, malate and aspartate is reflected in the decreased pool sizes, while a similar fraction of the pool is labeled by carbon derived from glutamate (Fig. 7G). Upon the second turn, a greater difference in the fractional $^{13}C_2$ labeled form is observed, again demonstrating reduced rate of TCA cycling upon *Hk2* deletion. Each of these patterns is mirrored in citrate/isocitrate (Fig. 7G).

Interestingly, we observed an increase in $^{13}C_5$- labeled citrate derived from U-$^{13}C_5$ Gln in the absence of HK2 (Fig. 7H), indicating reductive carboxylation is a larger contributor to the citrate pool in *Hk2* deleted cells. Consistent with increased $^{13}C_5$ citrate derived from reductive carboxylation, we observe a higher fraction of AcCoA in cells fed with U-$^{13}C_5$ Gln (Figs 7I, and S5G). Taken together with the finding that glycolytic contribution to the AcCoA pool is decreased, these results indicate that in the absence of HK2, reductive carboxylation partially compensates for the impaired glycolytic flux into citrate, AcCoA, and presumably fatty acid biosynthesis.

Taken together these results suggest that the TCA cycle is attenuated in the absence of HK2. Corresponding reductions in citrate abundance – derived from Glc and TCA cycle intermediates derived from Gln could be both a cause and a consequence of reduced Gln

incorporation, as anaplerosis and cataplerosis are always tightly matched to maintain TCA cycle carbon balance (Owen, 2002). Regardless of the explanation, these results suggest that the high HK2 expression induced by oncogenic Ras is an indirect determinant of Gln utilization. Therefore, it is possible that proliferation of oncogenic Ras-transformed cells in which *Hk2* is deleted is not further inhibited by Gln restriction due to a reduced anaplerotic role for Gln-derived carbon in these cells.

Discussion

Signature alterations in the metabolism of cancer cells have been recognized for over three-quarters of a century (Robey and Hay, 2009; Vander Heiden et al., 2009). Since the high flux of glucose utilization distinguishes many cancer cells from their normal counterparts, many of these studies provide rationales for targeting certain glycolytic enzymes for cancer therapy. However, because of the fundamental biological importance of glycolysis in normal metabolic homeostasis, concerns arise regarding potential adverse homeostatic consequences of targeting specific glycolytic enzymes in a systemic manner (Cheong et al., 2012). Selective cancer-associated expression of specific isoforms of certain glycolytic enzymes could render these enzymes potential selective targets for cancer therapy, if their expression is critical for the neoplastic phenotype. Amongst all these potential targets, the hexokinase isoform, HK2, could be an ideal target. HK2 is highly expressed in many cancers (Shinohara et al., 1994), and although it is abundantly expressed in embryonic tissues, it constitutes the predominant hexokinase isoform in only a limited number of adult tissues. In contrast, the HK1 isoform is ubiquitously expressed and constitutes the major hexokinase in most normal adult tissues (Wilson, 1995; Wilson, 2003).

Previous studies have demonstrated the ability of RNAi-mediated *HK2* silencing to inhibit tumor growth in a xenograft model of glioblastoma (Wolf et al., 2011). However it is unknown whether these results can be extrapolated to other forms of cancer, and the specific contributions of – and requirements for – HK2 and the other major hexokinase isoform, HK1, in both tumor initiation and maintenance are incompletely understood. In addition, it is unknown whether systemic targeting of HK2 is a viable approach to treating cancer. The, studies described herein provided a successful demonstration of systemic glycolytic enzyme targeting for cancer therapy without adverse effects on either metabolic homeostasis or lifespan.

Except skeletal muscles all other adult mouse tissues that abundantly express HK2 also express relatively high levels of HK1, which might play a compensatory or redundant role in the absence of HK2. In addition, the ability of tissues such as myocardium and skeletal muscle to utilize fatty acids as an alternate energy substrate could buffer the metabolic impact of *Hk2* deletion in these tissues (Felig and Wahren, 1975). Since the deletion of *Hk2* by the inducible Cre is not complete, it is possible that the residual HK2 activity in skeletal muscles is sufficient to maintain normal glucose homeostasis under resting conditions and normal chow diet.

Notably, mice with 50% germ line deletion of *Hk2* do not have a marked change in fed glucose levels under normal chow diet (Heikkinen et al., 1999). However they display hyperinsulinemia under a high fat diet, and reduced endurance during exercise (Fueger et al., 2003). Nonetheless, the possibility that the phenotype observed in mice with 50% germ line deletion is exerted through a developmental defect cannot be completely excluded. Thus, adult mice with a conditional deletion of *Hk2* may not exert these phenotypes.

Our studies showed that HK2 expression is exclusively elevated in lung and breast cancers, while HK1 expression did not change significantly. Although when overexpressed HK1 can

compensate for the loss of HK2 to some extent, we found that the loss of HK2 was not followed by a compensatory elevated expression of HK1. The underlying molecular basis for selective HK2 overexpression in cancer cells is incompletely understood, but this observation may relate to the fact that HK1 is constitutively expressed in most normal tissues, whereas HK2 is the principal inducible isoform (Robey and Hay, 2006). Another plausible explanation for the selective induction of HK2 expression in tumor cells is that it might be more compatible for the intrinsic properties of cancer cells. Although HK1 and HK2 display very similar kinetics of metabolic activities some features of HK2, which distinguish it from HK1 may render it more suited to the versatile metabolic nature of cancer cells. For instance, unlike HK1, which has a single active catalytic domain in its carboxy-terminus, HK2 possesses two active catalytic domains in its amino- and carboxy- termini. The two catalytic domains of HK2 have different kinetics properties and thus may retain its activity under conditions that are inhibitory for the single catalytic domain of HK1 (Wilson, 2003).

The effect contribution of HK2 on the metabolism of $KRas^{G12D}$-NSCLC cells

Accumulating data suggest that the metabolites generated by the branched pathways are much more critical for cancer cells than glycolysis per-se (Vander Heiden et al., 2009). These metabolites are critical to support anabolic processes such as nucleic acids and lipid synthesis. Previous results showed that oncogenic Ras elevates ribonucleotides synthesis largely through the non-oxidative branch of the PPP (Ying et al., 2012). Our results show that in the absence of HK2 the diversion of glucose to ribonucleotides synthesis through the non-oxidative branch of the PPP in $KRas^{G12D}$-NSCLC cells is reduced (Fig. 8). Thus, the induction of HK2 expression by oncogenic Ras is critical for the accelerated ribonucleotides synthesis. The results also suggest that the diversion of glucose into the serine biosynthesis pathway is reduced in the absence of HK2 (Fig. 8). Metabolic serine flux can be quite high in cancer cells where increased serine biosynthesis has been appreciated for almost three decades (Kalhan and Hanson, 2012). The levels and activities of enzymes in this pathway are elevated in cancer cells, and found to be critical for cancer cells' maintenance (Locasale and Cantley, 2011; Possemato et al., 2011).

Finally, HK2 expression appears to be required for the efficient flow of carbons from glycolysis onto the TCA cycle as manifested by the reduced glucose derived acetyl-CoA and citrate, which could also affect the diversion of glucose into fatty acid synthesis (Fig. 8). In cancer cells and oncogenic Ras transformed cells TCA cycle intermediates, except citrate, are predominately derived from auxotrophic glutamine (DeBerardinis et al., 2007; Gaglio et al., 2011). *Hk2* deletion inhibits glutamine-derived carbon utilization in anaplerosis (Fig. 8), for a reason that is not immediately clear to us. However, it is possible that reduced glucose-derived citrate somehow contributes to the attenuation of the flux from glutamine to other TCA cycle intermediates. This is also manifested by the increase in the reductive carboxylation in the absence of HK2, possibly to compensate for the lack of citrate derived from glycolysis (Fig. 8).

In summary, HK2 plays a critical role in the diversion of glucose into pathways, which are required for the anabolic activities in cancer cells. Interestingly, it was shown and proposed previously that in cancer cells downstream glycolytic activities are attenuated in order to divert glucose into the branched pathways. Our results suggest that an increase in the most upstream step in glucose metabolism catalyzed by HK2 is also critical for diverting glucose into these pathways in cancer cells. Therefore, this could explain why cancer cells, in contrast to their normal counterparts, express high levels of HK2. The expression of HK1 is possibly sufficient for normal cell metabolism. The accelerated anabolic metabolism in cancer cells demands a robust hexokinase activity and therefore the induction of HK2 expression is required.

Future implications for cancer therapy

Our studies placed HK2 as a selective therapeutic target for NSCLC and breast cancer. Moreover, since it was shown that breast cancer metastasis to the brain is significantly associated with high HK2 expression with poor patient survival (Palmieri et al., 2009), it is possible that HK2 ablation would inhibit metastasis.

We had previously shown that mitochondrial hexokinases, HK1 and HK2, binding to mitochondria promotes cell survival (Gottlob et al., 2001; Majewski et al., 2004). Thus, it is expected that the ablation of HK2 would increase cell death. The results presented here, however, show that the deficiency of HK2 exerts cytostastic effect in vitro and in vivo. There are several possible reasons for why we did not observe an increase in cell death after HK2 ablation. First, the cells also express HK1, which could be sufficient to protect from cell death. Second, the experiments were done with established cell lines in which *Hk2* was either deleted or was stably knocked down, and thus it is possible that during the establishment of the cell lines, cells in which HK2 was ablated beyond a certain threshold level were eliminated. Supporting this possibility is the observation that upon a conditional knockdown of HK2, there was a significant increase in cell death although at low magnitude. Finally, we cannot completely rule out an increase in cell death because it might be technically difficult to observe low levels of cell death in vivo, especially if the dead cells are phagocytosized. Nevertheless, it is possible that the deficiency of HK2 will render cancer cells more susceptible to cell death by pro-apoptotic drugs. Notably, investigations on drug resistance phenotypes of breast cancer cells showed that upregulated glucose metabolism, and especially HK2 expression are associated with the chemoresistance phenotypes in breast cancer cells (Kaplan et al., 1990; Komurov et al., 2012; Lyon et al., 1988). Therefore, HK2 may be a genetic modifier of drug resistance that can be therapeutically exploited.

Taken together our results provided strong rationales for developing small molecules inhibitors of HK2 for cancer therapy. Perhaps the biggest challenge is to develop inhibitors that could preferentially target HK2 and not HK1. Although HK1 and HK2 are very similar to each other, they exhibit some specific properties that could be exploited for isoform specific inhibition. For instance, both HK1 and HK2 are inhibited to the same extent by their own product, G6P. However, inorganic phosphate antagonizes the inhibition of HK1 by G6P, while it increases the inhibition of HK2 by G6P (Wilson, 2003). Since an increase in intracellular inorganic phosphate is usually observed in high glycolytic cells, such as cancer cells, this property of HK2 could be exploited for the preferential inhibition of HK2 in cancer therapy.

Experimental Procedures

Mice stains

Hexokinase 2 conditional knockout ($Hk2^{flox/flox}$ *or* $Hk2^{f/f}$) mice were generated as described in Fig. S1A. $KRas^{LSL\text{-}G12D}$, and *MMTV-Neu-IRES-Cre* ($MMTV^{NIC}$) mice were described before (Jackson et al., 2001; Ranger et al., 2009). $KRas^{LA2\text{-}G12D}$ (Johnson et al., 2001) obtained from the NCI-Mouse Models of Human Cancer Consortium. $UBC^{CreERT2}$ and $MMTV^{NeuT}$ mice were purchased from the Jackson laboratory. Generations of other mice are detailed in Supplemental Material. All animal experiments were approved by the University of Illinois at Chicago institutional animal care and use committee.

Cell lines

NCI-H460, NCI-H1299, NCI-H727, NCI-H358, T47D, MDA-MB-453, BT474, LA2-1B, and LA2-2 cells were grown in RPMI-1640/10% FBS/1% pen-strep media. MCF-10A cells

were maintained in DMEM/F12 with the supplements. MDA-MB-231, 293FT, phoenix-ecotropic cells, and mouse embryonic fibroblasts (MEFs) were maintained in DMEM/10% FBS/1% pen-strep media. All the cell lines were grown at 37 °C, 5% CO_2 incubator unless otherwise mentioned.

Statistical analysis

Statistical analysis was done with unpaired Student's *t*-tests, survival curves were analyzed by log-rank test (Mantel-Cox) and data are expressed as SD or SEM as indicated in the figure legend. Unless otherwise indicated all the experiments were performed for at least three times.

Supplementary Material

Refer to Web version on PubMed Central for supplementary material.

Acknowledgments

We are indebted to Shengfang Jin (Agios Pharmaceuticals.) for her support, and for heroic efforts to coordinate the metabolomics studies. We thank Veronique Nogueira, Wan-Ni Yu, Xiao-ding Peng, Nilotpal Roy and other present and past Hay Lab members for various reagents and for their help and suggestions. We thank Pradip Raychaudhuri (UIC), Jonna Frasor (UIC) and Alejandro Sweet-Cordero (Stanford Univ.) for their generous gift of some of the cell lines used in this study.

This work was supported by VA Merit Award BX000733, by NIH grants AG016927 and CA090764, and in part by the University of Illinois at Chicago Center for Clinical and Translational Sciences Award Number ULRR029879, and grant from the Chicago Biomedical Consortium with support from The Searle Funds at The Chicago Community to N.H.. K.C.P. was supported by DOD pre-doctoral fellowship W81XWH-11-1-0006.

References

Cheong H, Lu C, Lindsten T, Thompson CB. Therapeutic targets in cancer cell metabolism and autophagy. Nat Biotechnol. 2012; 30:671–678. [PubMed: 22781696]

DeBerardinis RJ, Mancuso A, Daikhin E, Nissim I, Yudkoff M, Wehrli S, Thompson CB. Beyond aerobic glycolysis: transformed cells can engage in glutamine metabolism that exceeds the requirement for protein and nucleotide synthesis. Proc Natl Acad Sci U S A. 2007; 104:19345–19350. [PubMed: 18032601]

Felig P, Wahren J. Fuel homeostasis in exercise. N Engl J Med. 1975; 293:1078–1084. [PubMed: 1178025]

Fueger PT, Heikkinen S, Bracy DP, Malabanan CM, Pencek RR, Laakso M, Wasserman DH. Hexokinase II partial knockout impairs exercise-stimulated glucose uptake in oxidative muscles of mice. Am J Physiol Endocrinol Metab. 2003; 285:E958–963. [PubMed: 12865258]

Gaglio D, Metallo CM, Gameiro PA, Hiller K, Danna LS, Balestrieri C, Alberghina L, Stephanopoulos G, Chiaradonna F. Oncogenic K-Ras decouples glucose and glutamine metabolism to support cancer cell growth. Mol Syst Biol. 2011; 7:523. [PubMed: 21847114]

Gottlob K, Majewski N, Kennedy S, Kandel E, Robey RB, Hay N. Inhibition of early apoptotic events by Akt/PKB is dependent on the first committed step of glycolysis and mitochondrial hexokinase. Genes Dev. 2001; 15:1406–1418. [PubMed: 11390360]

Heikkinen S, Pietila M, Halmekyto M, Suppola S, Pirinen E, Deeb SS, Janne J, Laakso M. Hexokinase II-deficient mice. Prenatal death of homozygotes without disturbances in glucose tolerance in heterozygotes. J Biol Chem. 1999; 274:22517–22523. [PubMed: 10428828]

Jackson EL, Willis N, Mercer K, Bronson RT, Crowley D, Montoya R, Jacks T, Tuveson DA. Analysis of lung tumor initiation and progression using conditional expression of oncogenic K-ras. Genes Dev. 2001; 15:3243–3248. [PubMed: 11751630]

Johnson L, Mercer K, Greenbaum D, Bronson RT, Crowley D, Tuveson DA, Jacks T. Somatic activation of the K-ras oncogene causes early onset lung cancer in mice. Nature. 2001; 410:1111–1116. [PubMed: 11323676]

Kalhan SC, Hanson RW. Resurgence of serine: an often neglected but indispensable amino Acid. J Biol Chem. 2012; 287:19786–19791. [PubMed: 22566694]

Kaplan O, Navon G, Lyon RC, Faustino PJ, Straka EJ, Cohen JS. Effects of 2-deoxyglucose on drug-sensitive and drug-resistant human breast cancer cells: toxicity and magnetic resonance spectroscopy studies of metabolism. Cancer Res. 1990; 50:544–551. [PubMed: 2297696]

Lee WN, Boros LG, Puigjaner J, Bassilian S, Lim S, Cascante M. Mass isotopomer study of the nonoxidative pathways of the pentose cycle with [1,2-13C2]glucose. Am J Physiol. 1998; 274:E843–851. [PubMed: 9612242]

Locasale JW, Cantley LC. Genetic selection for enhanced serine metabolism in cancer development. Cell Cycle. 2011; 10:3812–3813. [PubMed: 22064516]

Lunt SY, Vander Heiden MG. Aerobic glycolysis: meeting the metabolic requirements of cell proliferation. Annu Rev Cell Dev Biol. 2011; 27:441–464. [PubMed: 21985671]

Lyon RC, Cohen JS, Faustino PJ, Megnin F, Myers CE. Glucose metabolism in drug-sensitive and drug-resistant human breast cancer cells monitored by magnetic resonance spectroscopy. Cancer Res. 1988; 48:870–877. [PubMed: 3338082]

Majewski N, Nogueira V, Bhaskar P, Coy PE, Skeen JE, Gottlob K, Chandel NS, Thompson CB, Robey RB, Hay N. Hexokinase-mitochondria interaction mediated by Akt is required to inhibit apoptosis in the presence or absence of Bax and Bak. Mol Cell. 2004a; 16:819–830. [PubMed: 15574336]

Mathupala SP, Rempel A, Pedersen PL. Glucose catabolism in cancer cells: identification and characterization of a marked activation response of the type II hexokinase gene to hypoxic conditions. J Biol Chem. 2001; 276:43407–43412. [PubMed: 11557773]

Muller WJ, Sinn E, Pattengale PK, Wallace R, Leder P. Single-step induction of mammary adenocarcinoma in transgenic mice bearing the activated c-neu oncogene. Cell. 1988; 54:105–115. [PubMed: 2898299]

Nogueira V, Park Y, Chen CC, Xu PZ, Chen ML, Tonic I, Unterman T, Hay N. Akt determines replicative senescence and oxidative or oncogenic premature senescence and sensitizes cells to oxidative apoptosis. Cancer Cell. 2008; 14:458–470. [PubMed: 19061837]

Palmieri D, Fitzgerald D, Shreeve SM, Hua E, Bronder JL, Weil RJ, Davis S, Stark AM, Merino MJ, Kurek R, et al. Analyses of resected human brain metastases of breast cancer reveal the association between up-regulation of hexokinase 2 and poor prognosis. Mol Cancer Res. 2009; 7:1438–1445. [PubMed: 19723875]

Possemato R, Marks KM, Shaul YD, Pacold ME, Kim D, Birsoy K, Sethumadhavan S, Woo HK, Jang HG, Jha AK, et al. Functional genomics reveal that the serine synthesis pathway is essential in breast cancer. Nature. 2011; 476:346–350. [PubMed: 21760589]

Ranger JJ, Levy DE, Shahalizadeh S, Hallett M, Muller WJ. Identification of a Stat3-dependent transcription regulatory network involved in metastatic progression. Cancer Res. 2009; 69:6823–6830. [PubMed: 19690134]

Robey RB, Hay N. Mitochondrial hexokinases, novel mediators of the antiapoptotic effects of growth factors and Akt. Oncogene. 2006; 25:4683–4696. [PubMed: 16892082]

Robey RB, Hay N. Is Akt the “Warburg kinase”?-Akt-energy metabolism nteractions and oncogenesis. Semin Cancer Biol. 2009; 19:25–31. [PubMed: 19130886]

Ruzankina Y, Pinzon-Guzman C, Asare A, Ong T, Pontano L, Cotsarelis G, Zediak VP, Velez M, Bhandoola A, Brown EJ. Deletion of the developmentally essential gene ATR in adult mice leads to age-related phenotypes and stem cell loss. Cell Stem Cell. 2007; 1:113–126. [PubMed: 18371340]

Schulze A, Harris AL. How cancer metabolism is tuned for proliferation and vulnerable to disruption. Nature. 2012; 491:364–373. [PubMed: 23151579]

Shedden K, Taylor JM, Enkemann SA, Tsao MS, Yeatman TJ, Gerald WL, Eschrich S, Jurisica I, Giordano TJ, Misek DE, et al. Gene expression-based survival prediction in lung adenocarcinoma: a multi-site, blinded validation study. Nat Med. 2008; 14:822–827. [PubMed: 18641660]

Shinohara Y, Yamamoto K, Kogure K, Ichihara J, Terada H. Steady state transcript levels of the type II hexokinase and type 1 glucose transporter in human tumor cell lines. Cancer Lett. 1994; 82:27–32. [PubMed: 7518342]

Skeen JE, Bhaskar PT, Chen CC, Chen WS, Peng XD, Nogueira V, Hahn-Windgassen A, Kiyokawa H, Hay N. Akt deficiency impairs normal cell proliferation and suppresses oncogenesis in a p53-independent and mTORC1-dependent manner. Cancer Cell. 2006; 10:269–280. [PubMed: 17045205]

Ursini-Siegel J, Hardy WR, Zuo D, Lam SH, Sanguin-Gendreau V, Cardiff RD, Pawson T, Muller WJ. ShcA signalling is essential for tumour progression in mouse models of human breast cancer. EMBO J. 2008; 27:910–920. [PubMed: 18273058]

van de Vijver MJ, He YD, van't Veer LJ, Dai H, Hart AA, Voskuil DW, Schreiber GJ, Peterse JL, Roberts C, Marton MJ, et al. A gene-expression signature as a predictor of survival in breast cancer. N Engl J Med. 2002; 347:1999–2009. [PubMed: 12490681]

Vander Heiden MG, Cantley LC, Thompson CB. Understanding the Warburg effect: the metabolic requirements of cell proliferation. Science. 2009; 324:1029–1033. [PubMed: 19460998]

Wilson JE. Hexokinases. Rev Physiol Biochem Pharmacol. 1995; 126:65–198. [PubMed: 7886381]

Wilson JE. Isozymes of mammalian hexokinase: structure, subcellular localization and metabolic function. J Exp Biol. 2003; 206:2049–2057. [PubMed: 12756287]

Wolf A, Agnihotri S, Micallef J, Mukherjee J, Sabha N, Cairns R, Hawkins C, Guha A. Hexokinase 2 is a key mediator of aerobic glycolysis and promotes tumor growth in human glioblastoma multiforme. J Exp Med. 2011; 208:313–326. [PubMed: 21242296]

Ying H, Kimmelman AC, Lyssiotis CA, Hua S, Chu GC, Fletcher-Sananikone E, Locasale JW, Son J, Zhang H, Coloff JL, et al. Oncogenic Kras maintains pancreatic tumors through regulation of anabolic glucose metabolism. Cell. 2012; 149:656–670. [PubMed: 22541435]

Significance

The feasibility of systemic targeting glycolytic enzymes for cancer therapy is unproven, but hexokinases, which catalyze the first committed step of glucose metabolism, are attractive candidate targets for such intervention. Targeting HK2, which is highly expressed in glycolytic cancer cells and not in normal cells could selectively target cancer cells. Using genetic approaches we showed that HK2 is required for tumor initiation and maintenance, and its deletion is therapeutic for cancer. To emulate drug therapy we showed that systemic whole body deletion of *Hk2* in the mouse is feasible and that it selectively targets cancer cells. Thus, we provided a proof of concept, using genetic approaches, that HK2 is an attractive target for cancer therapy.

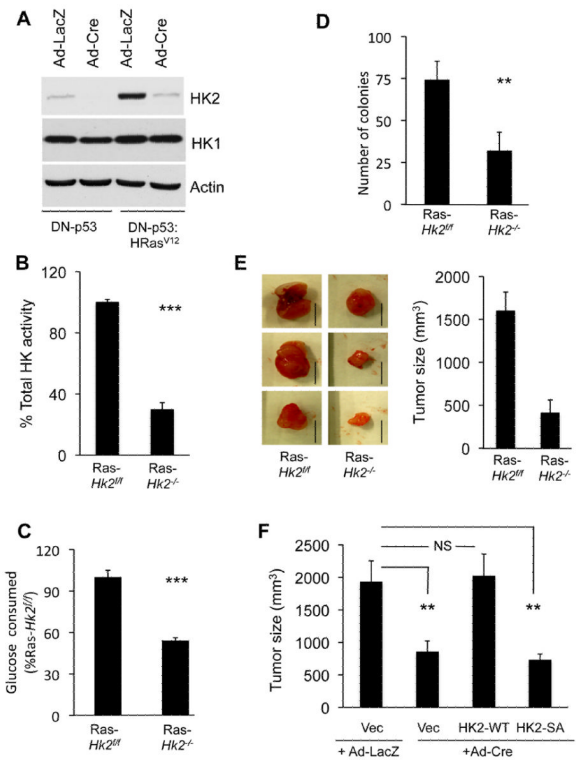

Figure 1. HK2 is required for oncogenic transformation

A. Immortalized *Hk2*$^{f/f}$ MEFs following infection with either Ad-Cre or Ad-LacZ, as a control, were established and stably infected with a retrovirus expressing oncogenic HRas^{V12}. Cell extracts were subjected to immunoblotting with anti-HK2 or anti-HK1 antibodies. Control undeleted cells are denoted *Hk2*$^{f/f}$ and *Hk2* deleted cells are denoted *Hk2*$^{-/-}$. **B**. Relative total hexokinase activity in Ras-transformed *Hk2*$^{f/f}$ and *Hk2*$^{-/-}$ MEFs. **C**. Relative glucose consumption in Ras-transformed *Hk2*$^{f/f}$ and *Hk2*$^{-/-}$ MEFs. Data represent the percentage of glucose consumed by Ras-transformed *Hk2*$^{-/-}$ MEFs as compared to Ras-transformed *Hk2*$^{f/f}$ MEFs after of culturing for 18h, and after adjusting for cell number. **D**. Average number of colonies generated by Ras transformed *Hk2*$^{f/f}$ and *Hk2*$^{-/-}$ MEFs after six weeks growth on soft-agar. **E**. The effect of *Hk2* deletion on tumorigenesis in vivo. Ras-transformed *Hk2*$^{f/f}$ and *Hk2*$^{-/-}$ MEFs were injected subcutaneously into athymic nude mice, and tumor size was calculated. Left panel showed representative tumor images of Ras-transformed *Hk2*$^{f/f}$ and *Hk2*$^{-/-}$ MEFs (Scale bars: 1 cm). Right panel show the average tumor size formed by Ras-transformed *Hk2*$^{f/f}$ and *Hk2*$^{-/-}$ MEFs. (n=4 tumors per each cell type). **F**. The requirement of HK2 activity for tumorigenesis in vivo. Ras-transformed *Hk2*$^{-/-}$ MEFs stably expressing WT or kinase-dead HK2, and Ras-transformed *Hk2*$^{f/f}$ or *Hk2*$^{-/-}$ control MEFs were subjected to tumorigenesis in vivo as described in (E). Tumor size was calculated when tumor size of control Ras-transformed *Hk2*$^{f/f}$ MEFs reached approximately 2cm^3. (n=4 tumors per each cell type). The data presented in Figs. B–F are expressed as ± SEM where ***, ** and * represent p≤ 0.001, 0.01 and 0.05 respectively. See also Fig. S1.

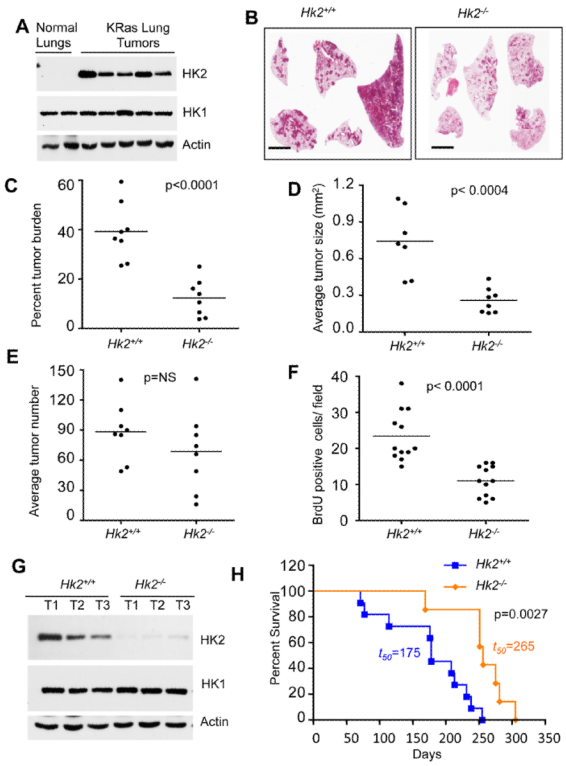

Figure 2. HK2 is required for the development of oncogenic KRas-driven NSCLC in mice, and its deletion extends the lifespan of these mice

A. Tissue lysates from lungs of control $KRas^{LSL\text{-}G12D}$ mice or from tumors in lungs of $KRas^{LSL\text{-}G12D}$ mice after exposure to Ad-Cre were subjected to immunoblotting with anti-HK2 or anti-HK1 antibodies. Ad-Cre treated $KRas^{LSL\text{-}G12D}$ and $KRas^{LSL\text{-}G12D}$;$Hk2^{f/f}$ mice are denoted as $Hk2^{+/+}$ and $Hk2^{-/-}$ respectively. **B**. Sixteen weeks after Cre instillation to induce lung tumors, lung sections were subjected to H&E staining (scale bar 4mm). **C**. Percentage tumor burden calculated from the H&E stained sections of tumor bearing lungs from $KRas^{LSL\text{-}G12D}$ mice (n=8) or $KRas^{LSL\text{-}G12D}$;$Hk2^{f/f}$ mice (n=8). **D**. Average tumor size per lungs of $KRas^{LSL\text{-}G12D}$ (n=7) or $KRas^{LSL\text{-}G12D}$;$Hk2^{f/f}$ (n=8) mice. **E**. Tumors number calculated from the H&E stained sections of tumor bearing lungs from $KRas^{LSL\text{-}G12D}$ (n=8) or $KRas^{LSL\text{-}G12D}$;$Hk2^{f/f}$ (n=8) mice. **F**. Average number of BrdU positive cells per field as calculated from 40X magnification of tumor sections. At least ten fields of $KRas^{LSL\text{-}G12D}$ or $KRas^{LSL\text{-}G12D}$;$Hk2^{f/f}$ lungs from three different mice were used for this analysis. Data in Figs C–F are expressed as the mean ± SEM. **G**. Immunoblot showing HK2 and HK1 expression in tumors obtained from $KRas^{LSL\text{-}G12D}$ or $KRas^{LSL\text{-}G12D}$;$Hk2^{f/f}$ lungs. **H**. Kaplan-Meier survival curves of lung tumor bearing $KRas^{LSL\text{-}G12D}$ or $KRas^{LSL\text{-}G12D}$;$Hk2^{f/f}$ mice after exposure to Ad-Cre at 8 weeks of age (p values and median survival (*t=50*) for the indicated genotypes were calculated by log-rank test).

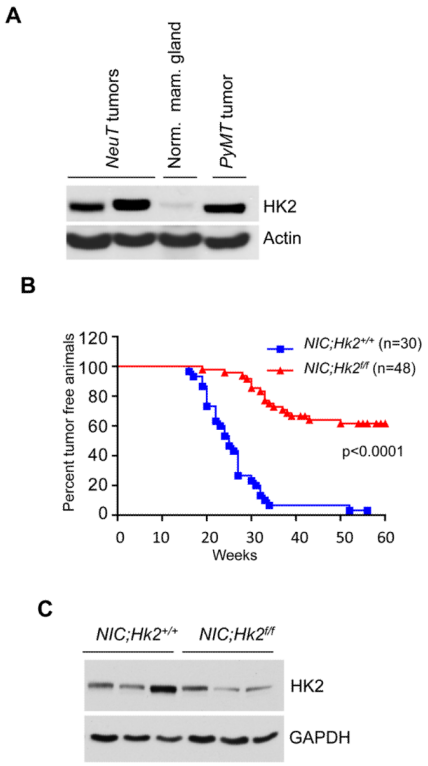

Figure 3. HK2 is required for the development of ErbB2/Neu-driven mammary tumors in mice

A. Immunoblot showing HK2 expression in tissue lysates from normal mammary gland or mammary gland tumors isolated from *MMTV*^{NeuT} and *MMTV*^{PyMT} mice. **B**. Kaplan-Meier curves of percentage tumor free survival of *MMTV*^{NIC} (*NIC;Hk2*$^{+/+}$) and *MMTV*^{NIC}*;Hk2*$^{f/f}$ (*NIC;Hk2*$^{f/f}$) mice. p value was calculated by log-rank test. **C**. Immunoblot showing HK2 expression in tumor lysates obtained from mice with the indicated genotypes.

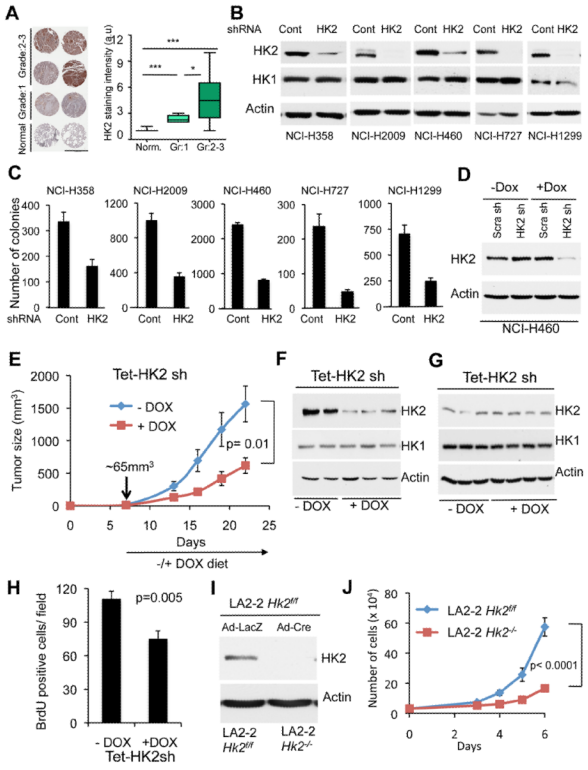

Figure 4. HK2 silencing reverses tumorigenesis of NSCLC cells in vitro and in-vivo

A. Left panel: Immunohistochemical staining of HK2 expression in representative human NSCLC patient samples tissue microarray (TMA) correlates with the pathological grade of the disease (scale bar 1mm). Right panel: Quantification of HK2 staining intensity in accordance with the pathological grade. TMA samples analyzed are; 20 non-tumor, 22 grade-1, 44 grade-2, and 14 grade-3. Box plots represent the 25th to 75th percentiles (boxes) with median and the whiskers represent the maximum and the minimum value. **B**. Immunoblot showing the level of HK2 and HK1 protein expression in a panel of human NSCLC cells stably expressing either shRNA targeting *HK2* or *LacZ* shRNA as control. **C**. Equal numbers of either control or HK2 knockdown cells were subjected to soft-agar assay, and colonies were counted after three weeks. Data are expressed as the mean of three independent experiments ± SEM ($p \leq 0.002$). **D**. Immunoblot showing HK2 protein level in NCI-H460 cells expressing an inducible control or HK2 shRNA. The cells were exposed to vehicle or 500ng/ml doxycycline (DOX) for 96 hrs prior to analysis. **E**. NCI-H460 cells (0.75×10^6) were injected subcutaneously into athymic nude mice. When tumor size reached ~65mm^3, mice were fed doxycycline containing diet (n=8) or normal chow diet (n=7), and tumor growth was followed until tumor size reached 1.5–2cm^3. **F**. At the end of the experiment described in E, tumor lysates were subjected to immunoblotting with anti-HK2 antibodies. **G**. Immunoblot showing HK2 protein levels in tumor lysates harvested one week after exposure to the DOX diet. **H**. BrdU incorporation in tumors one week after exposure to DOX diet. **I**. Deletion of *Hk2* in NSCLC cell line derived from *KRas$^{LA2\text{-}G12D}$;Hk2$^{f/f}$* mice. **J**. Cell proliferation after *Hk2* deletion in the NSCLC cell line derived from *KRas$^{LA2\text{-}G12D}$;Hk2$^{f/f}$* mice. Data presented in panels C, E, H and J are expressed as the mean ± SEM. See also Fig. S2.

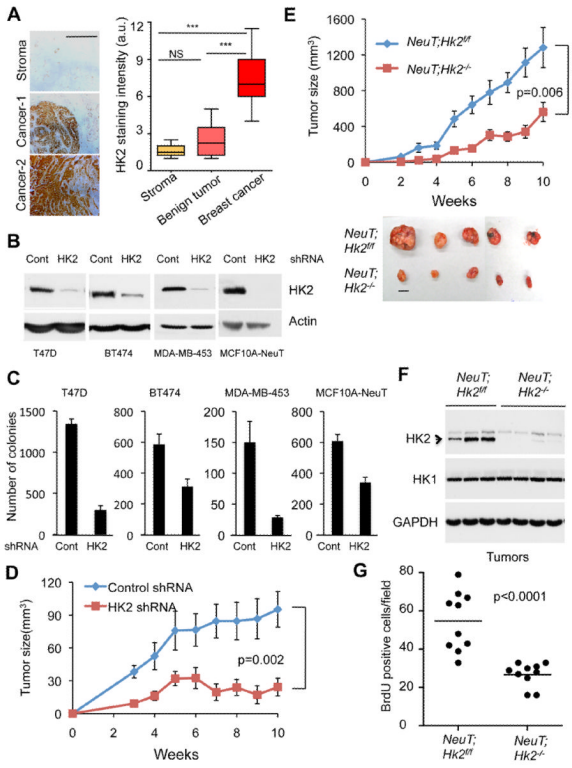

Figure 5. HK2 silencing reverses tumorigenesis of breast cancer cells in vitro and in vivo

A. Left panel: Representative images of immunohistochemical staining of HK2 in human breast cancer samples TMA, showing low expression in the stroma and benign tumors and high expression in cancer samples (scale bar 0.5mm). Right panel: Quantification of HK2 staining intensity in the stroma, benign tumors and cancer samples (Stroma (n=4, Benign (n=8), Tumor (n=15)). Box plots represent the 25th to 75th percentiles (boxes) with median and the whiskers represent the maximum and the minimum value. **B**. Immunoblot showing HK2 protein level in a panel of human breast cancer or transformed mammary cells stably expressing either shRNA targeting *HK2* or *LacZ* shRNA as control. **C**. Equal numbers of control or HK2 knockdown cells were subjected to soft-agar assay and colonies were counted after three weeks. Data is expressed as the mean of three independent experiments ± SEM ($p \leq 0.003$). **D**. Equal numbers of MDA-MB-453 cells stably expressing either HK2 shRNA or control shRNA were injected into the fat pad of the mammary glands of female athymic nude mice. Tumor growth was followed. **E**. Cells of cell line derived from a mammary tumor of $MMTV^{NeuT};Hk2^{f/f}$ mice were infected with either Ad-GFP or Ad-Cre-GFP to delete *Hk2* and to generate $NeuT;Hk2^{f/f}$ or $NeuT;Hk2^{-/-}$ cells. The cells were then injected orthotopically in female athymic nude mice (6 mice per group) and tumor growth was followed until tumor size reached approximately $2cm^3$. Bottom panel show representative images of tumors (scale bar 1cm). **F**. Immunoblot showing HK2 and HK1 protein levels in tumor protein lysates from individual tumors shown in E. **G**. Quantification of BrdU incorporation in tumor sections derived from the tumors described in E. The average number of BrdU positive cells per field was calculated from (40X magnification) of the tumor tissue sections. At least ten fields from three different tumors per each mouse genotype were used for the quantification. The data in Fig. 5D, 5E and 5G are expressed as the mean ± SEM. See also Fig. S3.

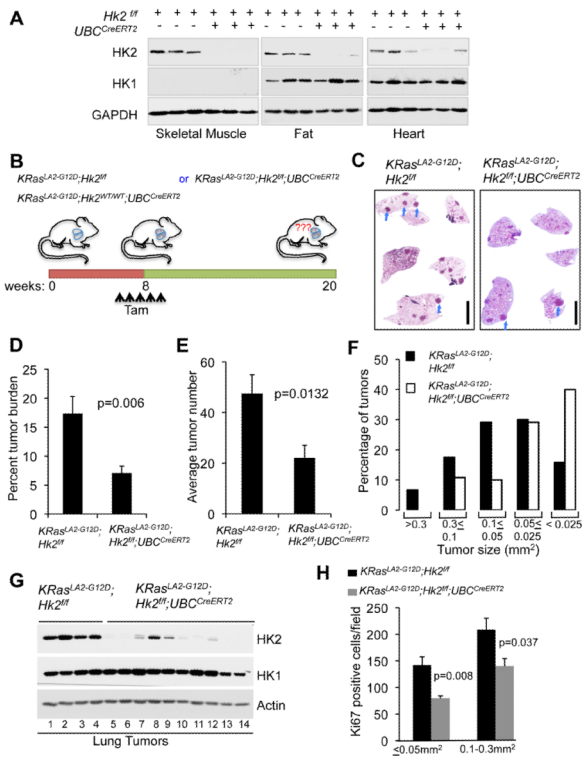

Figure 6. Systemic deletion of *Hk2* in the mouse is therapeutic for oncogenic KRas-driven NSCLC

A. Immunoblot showing HK2 and HK1 protein expression in tissues isolated from either $Hk2^{f/f}$ or $Hk2^{f/f}$;$UBC^{CreERT2}$ mice two weeks after final tamoxifen injection. **B**. Schematic illustration of the experiment described in C–H. **C**. Representative images of H&E staining of whole-mount lung sections prepared from either $KRas^{LA2\text{-}G12D}$;$Hk2^{f/f}$ or $KRas^{LA2\text{-}G12D}$;$Hk2^{f/f}$;$UBC^{CreERT2}$ lungs, 12 weeks after injection of tamoxifen at 8 weeks of age. Individual tumors are indicated by arrows (scale bar 4mm). **D**. Percentage tumor burden as calculated from the H&E sections of tumor bearing lungs from either $KRas^{LA2\text{-}G12D}$;$Hk2^{f/f}$ or $KRas^{LA2\text{-}G12D}$;$Hk2^{f/f}$;$UBC^{CreERT2}$ mice at 20 weeks of age and after injection of tamoxifen at 8 weeks of age (n=8 per group). **E**. Tumor numbers calculated from the H&E stained sections of tumor bearing lungs from either $KRas^{LA2\text{-}G12D}$;$Hk2^{f/f}$ or $KRas^{LA2\text{-}G12D}$;$Hk2^{f/f}$;$UBC^{CreERT2}$ mice (n=8 per group). **F**. Size distribution of tumors developed in the lungs of either $KRas^{LA2\text{-}G12D}$;$Hk2^{f/f}$ or $KRas^{LA2\text{-}G12D}$;$Hk2^{f/f}$;$UBC^{CreERT2}$ mice (n=6 per group). **G**. Immunoblot showing HK2 and HK1 protein levels in tumor lysates extracted at 20 weeks of age, and after tamoxifen injection at 8 weeks of age. Lanes 1–4- tumors were randomly selected for analysis; lanes 5,6 – tumor size < 0.025mm^2; lanes 7–9- tumor size 0.3–0.05mm^2; lanes 10–14-tumor size 0.05–0.025mm^2. **H**. Quantification of Ki67 staining of the same size groups of tumors derived from either $KRas^{LA2\text{-}G12D}$;$Hk2^{f/f}$ or $KRas^{LA2\text{-}G12D}$;$Hk2^{f/f}$;$UBC^{CreERT2}$ mice. Data presented in Figs. D, E and H are expressed as the mean ± SEM. See also Fig. S4.

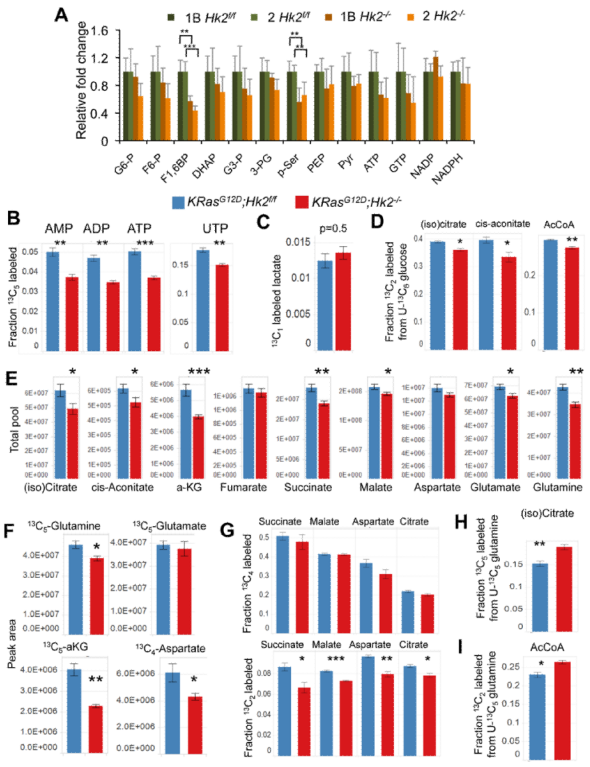

Figure 7. The effect of *Hk2* deletion in KRas^{G12D} NSCLC cells on the intracellular levels of metabolites derived from glucose or glutamine

A. Steady state levels of glycolytic metabolites in LA2-1B and LA2-2 cells in the presence or absence of HK2. Data are presented as fold changes of *Hk2*$^{f/f}$ versus *Hk2*$^{-/-}$ (n=5). **B.** Deletion of *Hk2* results in a decreased fraction of $^{13}C_5$ UTP and $^{13}C_5$ AMP, ADP and ATP from the PPP upon U-$^{13}C_6$ glucose feeding. **C.** No significant change between the fraction of labeled lactate containing $^{13}C_1$, or relative contribution of the oxidative PPP, upon deletion of *Hk2*. **D.** Contribution of glucose to the citrate / isocitrate, cis-aconitate and acetyl CoA pools is decreased by *Hk2* deletion, as observed by decreased $^{13}C_2$ species. **E.** Total pools of TCA cycle metabolites were averaged across all four labeling conditions (U-$^{12}C_6$ Glc; U-$^{13}C_6$ Glc; 1,2-$^{13}C_2$ Glc; U-$^{13}C_5$ Gln. Average of n=16 with SE. **F.** The $^{13}C_5$ or $^{13}C_4$ LC/MS/MS peak areas upon U-$^{13}C_5$ Gln feeding, **G.** Labeled $^{13}C_4$ (upper panel) and $^{13}C_2$ (bottom panel) succinate, malate, aspartate, and citrate derived from glutamine. **H.** Citrate/ isocitrate pools from reductive carboxylation upon *Hk2* deletion. **I.** AcCoA pools from reductive carboxylation upon *Hk2* deletion. A–I. Unless otherwise noted, values are an average of n=4 with SE, 2 hours post media switch (p values for A–I are: *p<0.05, **p<0.005, ***p<0.0005). See also Fig. S5.

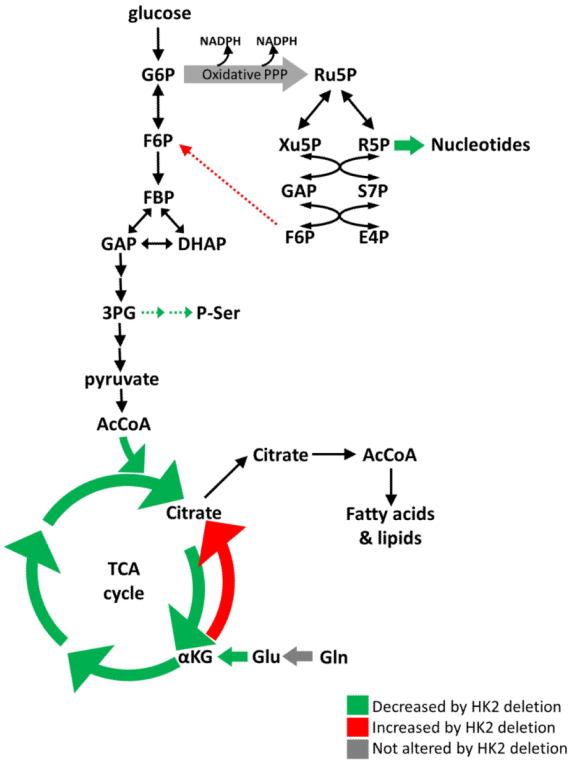

Figure 8.

Schematic illustration depicting metabolic changes induced by *Hk2* deletion in $KRas^{G12D}$-NSCLC cells. Decreased flux is green; increased flux is red; maintained flux is grey. Dashed arrows are predicted to be altered.